Article

Absolute Configuration, Conformation, and Circular Dichroism of Monocyclic Arene Dihydrodiol Metabolites: It is All Due to the Heteroatom Substituents

Jacek K. Gawronski, Marcin Kwit, Derek R. Boyd, Narain D. Sharma, John F. Malone, and Alex F. Drake

J. Am. Chem. Soc., **2005**, 127 (12), 4308-4319• DOI: 10.1021/ja042895b • Publication Date (Web): 08 March 2005

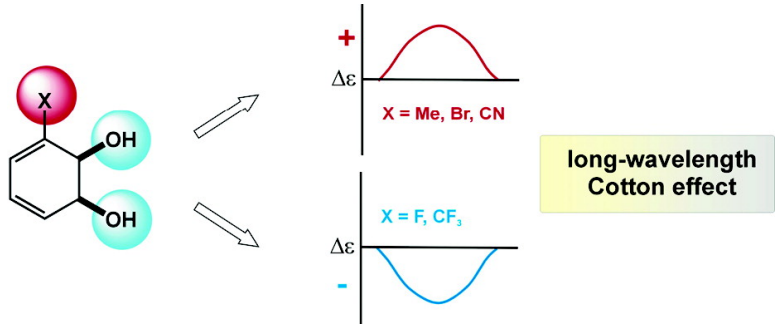

More About This Article

Additional resources and features associated with this article are available within the HTML version:

- Supporting Information
- Links to the 3 articles that cite this article, as of the time of this article download
- Access to high resolution figures
- Links to articles and content related to this article
- Copyright permission to reproduce figures and/or text from this article

View the Full Text HTML

J|A|C|S
ARTICLES
Published on Web 03/08/2005

Absolute Configuration, Conformation, and Circular Dichroism of Monocyclic Arene Dihydrodiol Metabolites: It is All Due to the Heteroatom Substituents

Jacek K. Gawronski,*,† Marcin Kwit,† Derek R. Boyd,‡ Narain D. Sharma,‡ John F. Malone,‡ and Alex F. Drake§

Contribution from the Department of Chemistry, A. Mickiewicz University, 60-780 Poznan, Poland, Centre for Theory and Application of Catalysis, School of Chemistry, The Queen's University of Belfast, Belfast BT9 5AG, U.K., and Department of Pharmacy, King's College London, Strand, London WC2R 2LS, U.K.

Received November 24, 2004; E-mail: gawronsk@amu.edu.pl

Abstract: Absolute configurations and conformations of selected *cis*-1,2-dihydrodiols, isolated from bacterial enzyme-catalyzed arene dihydroxylation, have been examined by comparison of experimental and DFT-calculated CD spectra and confrontation with the results of X-ray diffraction studies in the crystalline phase. The equilibrium between the diene *P* and *M* conformers in *cis*-dihydrodiols is strongly dependent on the intramolecular OH−OH, OH−π, and OH−F hydrogen bonding pattern and is crucial in determining the sign and magnitude of the long-wavelength diene $\pi-\pi^*$ transition Cotton effect. The differences originate from a dominant contribution of either *P*-helical (**1b**, X = Me) or *M*-helical conformers (**1d**, X = F), or are due to *M* and *P* low-energy conformers, both contributing a positive rotational strength (**1c**, X = Br). Computations show that *cis*-dihydrodiol **1e** (X = CF_3) has only one *M* conformer stabilized by an intramolecular O−H···F hydrogen bond. *cis*-Dihydrodiol **1f** (X = CN) shows a Cotton effect of the sign opposite to the sense of helicity of the dominating conformer. The results of the computations highlight the inadequacy of the *Diene Helicity Rule* and the *Allylic Chirality Rule* to correlate observed Cotton effects with dihydrodiol absolute configuration. A reliable model is presented to predict the absolute configuration of substituted benzene dihydrodiol derivatives from CD spectra, based on the confrontation of DFT-computed and experimental CD spectra. For 3-alkyl derivatives, a simple noncomputational model is offered, which is based on the contributions of the allylic hydroxy groups and the diene core in *P* and *M* conformers.

1. Introduction

Several oxidative metabolic pathways are available for the biodegradation of monocyclic aromatic rings **A** in the environment (Scheme 1).[1a−f] Prokaryotic (bacterial) metabolism often occurs via initially formed *cis*-dihydrodiol derivatives **B** resulting from regio- and stereoselective ring hydroxylating toluene dioxygenase-catalyzed (TDO-catalyzed) *cis*-dihydroxylation at the 2,3-bond of a monosubstituted benzene ring **A**.[1a−c] This metabolic pathway has been studied extensively using mutant and recombinant bacterial strains containing the TDO enzyme, and >50 examples of *cis*-1,2-dihydrodiol derivatives **B** of monosubstituted benzene rings **A** have been isolated.[1a−c] TDO-catalyzed oxidation of arene **A** results in a remarkable degree of regioselectivity (yielding *cis*-dihydrodiol **B** exclusively) and stereoselectivity (yielding the (1*S*) enantiomer of diol **B** exclusively in all cases with one exception, X = F) (Scheme 1).

Eukaryotic metabolism (fungi, animals, plants) often occurs via monooxygenase-catalyzed (CYP-450) epoxidation of the monosubstituted arene ring **A**. Regioselectivity can often be variable yielding different arene oxide regioisomers **C** and the corresponding *trans*-dihydrodiols **D** after epoxide hydrolase-catalyzed hydrolysis. Although a greater degree of regioselectivity has been observed in fungal oxidations, where a preference appears to be found for epoxidation at the 1,2- (X = CO_2Me)[2a] or 2,3-bonds (X = Cl and Br)[2b] of monosubstituted benzenes **A**, in mammalian liver metabolism, where a wide range of CYP-450 enzymes is available, the regioselectivity is lower. The metabolites **C** may then result from epoxidation at each of the 1,2-, 2,3-, and 3,4-bonds of monosubstituted benzenes **A** to yield the corresponding arene oxides **C**.[1d−f,3] Relatively few substituted benzene oxides **C**[2a] and *trans*-dihydrodiols **D**[4,5a−c] have

† A. Mickiewicz University.
‡ The Queen's University of Belfast.
§ King's College London.

(1) (a) Boyd, D. R.; Sheldrake, G. N. *Nat. Prod Rep*. **1998**, *15*, 309−324. (b) Hudlicky, T.; Gonzalez, D.; Gibson, D. T. *Aldrichimica Acta* **1999**, *32*, 35−62. (c) Johnson, R. A. *Org. React*. **2004**, *63*, 117−264. (d) Guengerich, F. P. *Pharmacol. Ther*. **1992**, *54*, 17−61. (e) Cerniglia, C. E. J. *Ind. Microbiol. Biotechnol*. **1997**, *19*, 324−333. (f) Boyd, D. R.; Sharma, N. D. *J. Mol. Catal. B* **2002**, *19*−*20*, 31−42.

(2) (a) Boyd, D. R.; Sharma, N. D.; Harrison, J. S.; Hamilton, J. T. D.; Harper, D. B.; McRoberts, W. C. *J. Chem. Soc., Chem. Commun*. **2000**, 2151−2152. (b) Auret, B. J.; Balani, S. K.; Boyd, D. R.; Greene, R. M. E.; Berchtold, G. A.; *J. Chem. Soc., Perkin Trans. 1* **1984**, 2659−2664.

(3) Boyd, D. R.; Sharma, N. D. *Chem. Soc. Rev*. **1996**, *25*, 289−296.

10.1021/ja042895b CCC: $30.25

Scheme 1. Oxidative Metabolism of Arenes in Prokaryotic and Eukaryotic Metabolism

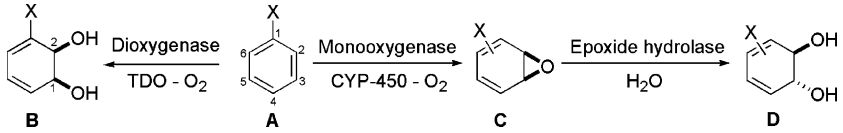

been isolated via biocatalysis. Chemoenzymatic methods using enantiopure *cis*-dihydrodiols **B** have, however, been used to obtain the corresponding racemic benzene oxides **C**[6] and *trans*-dihydrodiols **D**.[7] *trans*-Dihydrodiols are available also by chemical methods.[8,9]

The 1,3-cyclohexadiene chromophore is common to both the *cis*-**B** and *trans*-dihydrodiol (**D**) xenobiotic metabolites of monosubstituted benzene substrates (**A**) and is also frequently encountered in the structures of secondary metabolites (e.g., terpenes and steroids). A marked increase in the number of reports of the isolation and application of new enantiopure *cis*- and *trans*-dihydrodiols, containing the 1,3-cyclohexadiene moiety, has occurred over the past 15 years, and this has required the development of reliable methods for absolute configuration determination.[1a−f,3] Despite a continuing interest in the correlation of both absolute configuration (skew *s-cis*-diene) and substitution pattern with chiroptical phenomena (optical rotation, ORD, CD) over a period of 40 years, attempts to rationalize the experimental observations in a reliable manner have only met with partial success.[10] The original *Diene Helicity Rule*,[11] although successful for some *s-cis* terpenoid dienes, was unable to account for the long-wavelength Cotton effect of many other polycyclic conjugated *s-cis*-dienes.

To overcome the inadequacy of the *Diene Helicity Rule*, the concept of allylic axial substituent contributions to the determination of optical activity of conjugated dienes was proposed by Burgstahler and co-workers (*Allylic Axial Chirality Rule*).[12a,b] According to this concept, the sign of the long-wavelength Cotton effect of conjugated dienes is primarily due to the contribution of allylic axial substituents, such as alkyl groups. The sign of the contribution is determined by the helicity (+ or −) of the $C_{axial}-C_{allyl}-C{=}C$ bond system. A corollary of this rule is the low contribution of the helical conjugated diene chromophore to the rotational strength of the $\pi-\pi^*$ transition.

Certain substituents attached to one of the diene carbon atoms (e.g., the CN group) can cause sign reversal of the long-wavelength Cotton effect in the absence of any obvious structural change,[13] which again is not consistent with the *Diene Helicity Rule*. An experimental and theoretical study of 5-alkyl-1,3-cyclohexadienes by Lightner et al.[14] for the first time provided a dissection of the contributions of various structural elements to the cyclohexadiene 260 nm Cotton effect. The sign of the contribution due to the *s-cis*-diene moiety alone is opposite to that predicted by the *Diene Helicity Rule* for 5-alkyl-1,3-cyclohexadienes, and the sign and magnitude of the Cotton effect are apparently dominated by the contributions of axial allylic bonds (groups). Very recently, a more advanced ab initio calculation by Hansen and Bak[15] in the random phase approximation (RPA) using an aug-cc-pVTZ atomic basis set provided important confirmation of the earlier findings on the role of allylic substituents. The effects of the allylic methyl groups were found to follow a quadrant rule being almost additive, while contributions from axial substituents are significantly larger than those from equatorial groups.

The electronic spectroscopy of the planar *cis*-diene chromophore has been discussed based upon CD measurements.[16a] The $\pi-\pi^*$ nature of the transition centered around 275 nm has been confirmed. However, evidence for Rydberg and other valence transitions was reported at shorter wavelengths (250−200 nm). In the experience of the authors, the chiroptical properties of Rydberg and valence transitions are independent of each other and are effectively additive.[16b] The solvent behavior of the CD spectra of the *cis*-diene diols presented here preclude the presence of Rydberg transitions at wavelengths above 250 nm. CD spectra below 250 nm are generally more difficult to interpret, being the result of other valence transitions, Rydberg transitions, and conformational lability.

The chiroptical properties of conjugated dienes with allylic hydroxy substituents have been the subject of relatively few studies. *trans*-1,2-Dihydroxy-3,5-cyclohexadiene (**D**, X = H) is one of the initial intermediates in benzene metabolism, formed through the enzyme-catalyzed hydration of benzene oxide.[17] An experimental study, including variable temperature CD spectroscopy, has shown that both diequatorial and diaxial conform-

(4) Jerina, D. M.; Ziffer, H.; Daly, J. W. *J. Am. Chem. Soc*. **1970**, *92*, 1056−1061.
(5) (a) Müller, R.; Breuer, M.; Wagener, A.; Schmidt, K.; Leistner, E. *Microbiology* **1996**, *142*, 1005−1012. (b) Franke, D.; Sprenger, G. A.; Müller, R. *Angew. Chem., Int. Ed.* **2001**, *40*, 555−557. (c) Lorbach, V.; Franke, D.; Nieger, M.; Müller, R. *J. Chem. Soc., Chem. Commun*. **2002**, 494−495.
(6) Boyd, D. R.; Sharma, N. D.; Dalton, H.; Clarke, D. A. *J. Chem. Soc., Chem. Commun*. **1996**, 45−46.
(7) Boyd, D. R.; Sharma, N. D.; O'Dowd, C.; Hempenstall, F. *J. Chem. Soc., Chem. Commun*. **2000**, 2151−2152.
(8) (a)Chiasson, B. A.; Berchtold, G. A. *J. Am. Chem. Soc*. **1974**, *96*, 2898−2901. (b) DeMarinis, R. M.; Filer, C. N.; Waraszkiewicz, S. M.; Berchtold, G. A. *J. Am. Chem. Soc.* **1974**, *96*, 1193−1197.
(9) Hentemann, M.; Fuchs, P. L. *Org. Lett.* **1999**, *1*, 355−357.
(10) For recent reviews, see: (a) Gawronski, J. *Houben−Weyl Methods of Organic Chemistry*, 4th ed.; G. Thieme: Stuttgart, 1995; Vol. E21a, pp 499−533. (b) Salvadori, P.; Rosini, C.; Di Bari, L. In *The Chemistry of Dienes and Polyenes*; Rapoport, Z., Ed.; J. Wiley: New York, 1997; Vol. 1, pp 111−147. (c) Gawronski, J. In *Circular Dichroism: Principles and Applications*; Berova, N., Nakanishi, K., Woody, R. W., Eds.; Wiley-VCH: New York, 2000; pp 305−335.
(11) Moscowitz, A.; Charney, E.; Weiss, U.; Ziffer, H. *J. Am. Chem. Soc.* **1961**, *83*, 4661−4663.
(12) (a) Burgstahler, A. W.; Barkhurst, R. C. *J. Am. Chem. Soc.* **1970**, *92*, 7601−7603. (b) Burgstahler, A. W.; Weigel, L. O.; Gawronski, J. K. *J. Am. Chem. Soc.* **1976**, *98*, 3015−3016.
(13) Lessard, J.; Ruest, L.; Engel, Ch. R. *Can. J. Chem.* **1972**, *50*, 1433−1437 and references therein.
(14) Lightner, D. A.; Bouman, T. D.; Gawronski, J. K.; Gawronska, K.; Chappuis, J. L.; Crist, B. V.; Hansen, A. E. *J. Am. Chem. Soc.* **1981**, *103*, 5314−5327.
(15) Hansen, A. E.; Bak, K. L. *J. Phys. Chem. A* **2000**, *104*, 11362−11370.
(16) (a) Browne, A. R.; Drake, A. F.; Kearney, F. R.; Mason, S. F.; Paquette, L. A. *J. Am. Chem. Soc.* **1983**, *105*, 6123−6129. (b) The absorption maximum wavelength of a Rydberg transition is very sensitive to pressure in the gas phase or "internal solvent pressure" in solution. The wavelength of maximum absorption of a valence transition is relatively insensitive to pressure (or solvent density). Going from the gas phase to solution, from high to low temperatures, or less dense to more dense solvents, Rydberg transitions move progressively and markedly to shorter wavelengths, even passing through a valence transition feature without disturbing the valence transition. The CD at any particular pressure is the sum of the CD of the Rydberg and the valence contributions as though the transitions were from different molecules. Oppositely signed CD components can produce different extents of overlap cancellation and apparent spectral changes.
(17) Snyder, R.; Longacre, S. L.; Witmer, C. M.; Docsis, J. J. In *Advances in Experimental Medicine and Biology: Biological Reactive Intermediates II/Chemical Mechanisms and Biological Effects*; Snyder, R., Park, D. V., Kocsis, J. J., Jollow, D. J., Gibson, C. G., Witmer, C. M., Eds; Plenum: New York, 1982; Vol. 136A, pp 245−256.

ers of **D** (X = H) produce a positive Cotton effect at 260 nm. The more stable conformer with equatorial hydroxy groups has a rotational strength one order of magnitude lower than that of the less stable diaxial conformer.[18]

The large pool of chiral (1*S*)-*cis*-1,2-dihydroxy-3,5-cyclohexadiene derivatives (**B**, Scheme 1), available through microbial oxidation of benzene derivatives,[1a−c] represents a formidable challenge for absolute configuration determination by chiroptical methods. Earlier studies of Ziffer et al.[19] on the absolute configuration determination of several benzene *cis*-dihydrodiols relied on the correlation of CD data within a narrow range of alkyl-substituted homologues as well as on chemical correlation and the application of the *Dibenzoate Exciton Chirality Rule* to hydrogenated molecules. In another study, an empirical correlation between CD spectra of *cis*-dihydrodiol tricarbonyliron complexes and absolute configuration has been proposed.[20] Apart from obvious shortcomings (e.g., preparation of such complexes), the sign of the long-wavelength Cotton effect in this instance depends not only on the absolute configuration but also on the polarity of the substituent X in dihydrodiol **B**.[20]

The enzymatic process involved in *cis*-dihydrodiol synthesis from monosubstituted benzene substrates **A**, with few exceptions, has been shown to be highly enantiospecific, leading to products **B** of the same absolute configuration regardless of the nature of substituent X in the aromatic ring.[1a−c] However, *cis*-dihydrodiols **B** obtained from benzene derivatives by incubation with *Pseudomonas putida* differ not only in magnitude but also in the sign of optical rotation, depending on the nature of substituent X.[21] The differences in optical rotation most probably originate from two sources: (i) the position of equilibria between *P* or *M* diene conformers, and (ii) the sign and magnitude of the rotational strength of each *P* or *M* conformer (see discussion below). We therefore decided to study the correlation between the absolute configuration/conformation and CD spectra by computation of the structure and rotational strengths of individual conformers of representative *cis*-dihydrodiols **B** bearing either nonpolar or polar substituents X. A major objective was to clarify the role of the hydroxy groups and other heteroatom substituents in hydrogen bond stabilization of the conformers as well as to determine their contribution to the rotational strength of individual conformers.

Methods based on density functional theory were found to be attractive in terms of accuracy and computational effort, which hold true not only for ground states but also for electronically excited states.[22−24] Nowadays, many different functionals are available in commercial software, but to the best of our knowledge, until now, no functionals have been designed explicitly for excited states. The time-dependent density functional theory (TD-DFT) method, in which excited-state properties are determined from the linear response of the molecules to an external continuous wave field, has became an important tool for the theoretical treatment of molecular electronic excitation spectra.[25−28] The TD-DFT method provides results that are more reliable than those obtained from Hartree−Fock (HF)-based methods or the configuration interactions with single excitations (CIS) method and allows the calculation of electronic excitation spectra (UV/VIS) and chiroptical properties.[29−34] Recently, Diedrich and Grimme have systematically investigated modern quantum chemical methods for prediction of electronic circular dichroism spectra.[35] Unfortunately, there are no "golden rules" for the combination of functional and basis set to obtain the best results in each case.

The most important quantity in CD spectroscopy is the rotatory strength (*R*), theoretically defined for a transition between states $|\Psi_0\rangle$ and $\langle Y_i|$ as

$$R_{0i} = \mathrm{Im}(\langle\Psi_0|\hat{\mu}|\Psi_i\rangle\langle\Psi_0|\hat{m}|\Psi_i\rangle) = |\vec{\mu}_{0i}|\bullet|\vec{m}_{0i}|\bullet\cos(\mu_{0i},\vec{m}_{0i})$$

where $\hat{\mu}$ and $\hat{m}$ are the electric and magnetic dipole operators, respectively. Because rotatory strengths are signed quantities, the electric and magnetic transition moments ($\vec{\mu}_{0i}$ and $\vec{m}_{0i}$, respectively), the angle between both moments as well as the excitation energies has to be determined with higher accuracy than in UV/VIS spectroscopy. There are no functionals explicitly designed as yet for the excited states; however, in the literature, there are at least two main approaches to address this issue. Stephens et al.[31] highly recommend a combination of a B3LYP hybrid functional with a large basis set augmented with diffuse functions (for example, aug-cc-pVTZ). Grimme and coworkers[35−37] use relatively smaller basis sets in combination with various hybrid functionals differing in a fraction of "exact" Hartree−Fock exchange (HFXC), or they combine density functional theory with the multireference configuration interaction method (DFT/MRCI). The most appropriate functional can be found experimentally by testing calculations of the excited states for model compounds. Fortunately, both approaches give results which can reproduce well the experimental data. This allows the use of TD-DFT calculations for predicting a priori the absolute configuration (or conformation) of chiral organic molecules as well as metal complexes.[38]

(18) Gawronski, J.; Gawronska, K.; Buczak, G.; Katrusiak, A.; Skowronek, P.; Suemune, H. *Tetrahedron: Asymmetry* **1996**, *7*, 301−306.
(19) (a) Ziffer, H.; Jerina, D. M.; Gibson, D. T.; Kobel, V. M. *J. Am. Chem. Soc.* **1973**, *95*, 4048−4049. (b) Ziffer, H.; Kabuto, K.; Gibson, D. T.; Kobal, V. M. *Tetrahedron* **1977**, *33*, 2491−2496.
(20) Stephenson, G. R.; Howard, P. W.; Taylor, S. C. *J. Chem. Soc., Chem. Commun.* **1991**, 127−129.
(21) Boyd, D. R.; Dorrity, M. R. J.; Hand, M. V.; Malone, J. F.; Sharma, N. D. *J. Am. Chem. Soc.* **1991**, *113*, 666−667.
(22) Koch, W.; Holthausen, M. C. *A Chemist's Guide to Density Functional Theory*; Wiley-VCH: Weinheim, Germany, 2000.
(23) Adamo, C.; di Matteo, A.; Barone, V. From Classical Density Functionals to Adiabatic Connection Methods. The State of the Art. In *Advances in Quantum Chemistry*; Löwdin, P.-O., Ed.; Academic Press: New York, 1999; Vol. 36.
(24) Geerlings, P.; De Proft, F.; Langenaeker, W. *Chem. Rev.* **2003**, *103*, 1793.
(25) Furche, F. *J. Chem. Phys.* **2001**, *114*, 5982.
(26) Casida, M. E.; Jamorski, C.; Casida, K. C.; Salahub, D. R. *J. Chem. Phys.* **1998**, *108*, 4439.
(27) Stratmann, E. R.; Scuseria, G. E.; Frisch, M. J. *J. Chem. Phys.* **1998**, *109*, 8218.
(28) (a) Runge, E.; Gross, E. K. U. *Phys. Chem. Lett*. **1984**, *52*, 997. (b) Gross, E. K. U.; Kohn, W. *Adv. Quantum Chem*. **1990**, *21*, 255. (c) Gross, E. K. U.; Dobson, J. F.; Petersilka, M. *Top. Curr. Chem.* **1996**, *181*, 81.
(29) Bauernschmitt, R.; Ahlrichs, R. *Chem. Phys. Lett.* **1996**, *256*, 454.
(30) Neiss, C.; Saalfrank, P.; Parac, M.; Grimme, S. *J. Phys. Chem. A* **2003**, *107*, 140.
(31) (a) Stephens, P. J.; McCann, D. M.; Devlin, F. J.; Cheeseman, J. R.; Frisch, M. J. *J. Am. Chem. Soc.* **2004**, *126*, 7514. (b) Stephens, P. J.; McCann, D. M.; Butkus, E.; Stončius, S.; Cheeseman, J. R.; Frisch, M. J. *J. Org. Chem.* **2004**, *69*, 1948.
(32) Autschbach, J.; Ziegler, T.; van Gisbergen, S. J. A.; Baerends, E. J. *J. Chem. Phys.* **2002**, *116*, 6930.
(33) Yabana, K.; Bertsch, G. F. *Phys. Rev. A* **1999**, *60*, 1271.
(34) Autschbach, J.; Patchkovskii, S.; Ziegler, T.; van Gisbergen, S. J. A.; Baerends, E. J. *J. Chem. Phys.* **2002**, *116*, 6930.
(35) Diedrich, C.; Grimme, S. *J. Phys. Chem. A* **2003**, *107*, 2524.
(36) Furche, F.; Ahlrichs, R.; Wachsmann, C.; Weber, E.; Sobanski, A.; Vögtle, F.; Grimme, S. *J. Am. Chem. Soc.* **2000**, *122*, 1717.
(37) Grimme, S.; Mennicke, W.; Vögtle, F.; Nieger, M. *J. Chem. Soc., Perkin Trans. 2* **1999**, 521.
(38) Autschbach, J.; Jorge, F. E.; Ziegler, T. *Inorg. Chem.* **2003**, *42*, 2867.

Chart 1

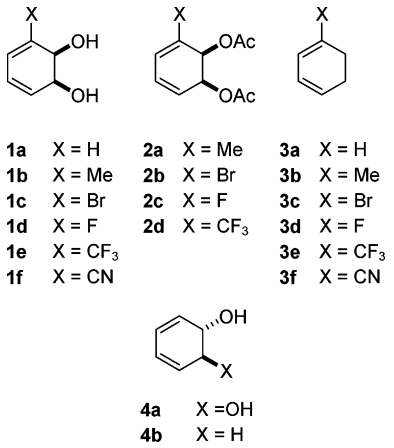

2. Materials and Methods

2.1. Source of Dihydrodiols. The enantiopure (1*S*)-*cis*-dihydrodiols of general structure **B** (hereupon identified individually as compounds **1b**−**1f**, Chart 1) have all been isolated as bacterial metabolites using the parent monosubstituted benzene substrates, the *P. putida* UV4 mutant strain, and the whole-cell biotransformation procedures reported earlier.[1a,39−41]

The methods used for the determination of enantiomeric excess values (>98% ee) and absolute configurations of the *cis*-dihydrodiols in the current study were as reported earlier.[21,39−42] These include (i) formation of cycloadducts with *N*-phenyltriazolinedione and NMR analysis of the corresponding diMTPA esters, (ii) chiral stationary phase HPLC, (iii) formation of chiral boronate derivatives and NMR analysis, (iv) X-ray crystallography, (v) CD spectroscopy, and (vi) stereochemical correlation.

2.2. Spectroscopy. UV and CD spectra were measured of ca. 5×10^{-3} M solutions in appropriate high-purity solvents in a 0.05 cm strain-free, fused-silica, cylindrical cell (Hellma) using a Jasco J700 spectropolarimeter. Data were processed according to Arvinte et al.,[43] allowing the simultaneous measurement of absorption and dichroism. The diols were only sparingly soluble in cyclohexane, and care was taken to ensure complete solubilization. The cyano-*cis*-diol **1f** was not sufficiently soluble in cyclohexane to allow reliable measurement.

2.3. Computational Methods. In our computations, all excited-state calculations have been performed based upon the ground-state geometries of single molecules with the use of a Gaussian program package.[44] Thus, the results correspond to vertical transitions, and the excitation energies can be compared with the band maxima in the experimental spectra. Rotatory strengths were calculated using length and velocity representations. According to Grimme, the length representation provides better results in most cases, compared to the velocity representation. Length and velocity rotatory strengths are equal and origin-independent at the complete basis set limit. In the present study, the differences between the length and velocity calculated values of rotatory strengths were quite small (see Supporting Information). The CD spectra were simulated by overlapping Gaussian functions for each transition according to the procedure described by Grimme et al.[35]

2.4. Conformational Analysis. Conformational analysis of the benzene *cis*-dihydrodiol **1a** was carried out in two ways. First, on the basis of the results obtained by a conformational search with the use of both MM3 molecular mechanics force field and AM1 Hamiltonian, the lowest-energy conformer of **1a(*P*)** was obtained.[45] This structure was further fully optimized using, at first, a hybrid functional B3LYP with a small basis set 6-31g(d) and then was reoptimized with the use of an enhanced basis set 6-31++g(d,p) and a B3LYP functional. A second systematic conformational search was carried out using a B3LYP functional and the large 6-311++g(d,p) basis set, starting from the structure optimized by the B3LYP/6-31++g(d,p) method, to find the relationship between the energy of the molecule and conformations of the hydroxy substituents. For this reason, torsion angles H−O−C*−H were rotated in 30° steps to give 144 different structures for **1a(*P*)**. A single point energy at the B3LYP/6-311+g(d,p) level was calculated for each structure, and this allowed the construction of the PES for **1a(*P*)**. From a total number of 144, those conformations having relative energies ranging from 0.0 to 1.5 kcal mol^{-1} were selected and fully optimized at the B3LYP/6-311++g(d,p)//B3LYP/6-31++g(d,p) level of theory. In the case of the **1a(*P*)** set of conformers, all optimized structures converged to the conformer representing the global energy minimum. For this structure, frequency calculations were carried out at the B3LYP/6-31++g(d,p) level of theory to establish that the conformation is stable. Due to the mirror symmetry of conformations **1a(*P*)** and **1a(*M*)**, the lowest-energy (*M*) conformer of **1a** was constructed from the lowest-energy (*P*) conformer of **1a**.

The lowest-energy *P* and *M* conformers of the achiral *cis*-dihydrodiol **1a** were then used as starting points for computing thermally accessible *P* and *M* conformers of the chiral *cis*-dihydrodiols **1b**−**1f**. First, the vinylic hydrogen atoms at C3 in conformers **1a(*P*)** and **1a(*M*)** were replaced by Me, Br, F, CF_3, or CN substituents to give *P* and *M* conformers of **1b**, **1c**, **1d**, **1e**, or **1f**, respectively. Then, full structure optimizations were performed for all compounds at the B3LYP/6-31++g(d,p) level, followed by a systematic conformational search at the B3LYP/6-311++g(d,p) level for each previously optimized structure, according to the procedure described for the conformational analysis of **1a(*P*)**. Molecules **1c**, **1d**, and **1f** were found to have one stable conformer of *P* helicity and two stable conformers of *M* helicity. In the case of diol **1e**, only one stable conformer of *M* helicity was found, whereas for compound **1b**, the stable conformers included one with *P* and one with *M* diene helicity.

The conformational search for *trans*-dihydrodiol **4a** was based upon the X-ray diffraction data.[18] For the diaxial conformer (*P*)-**4a**, OH···π interactions and C_2 symmetry were assumed. After geometry optimization at the B3LYP/6-31++g(d,p) level, systematic conformational search was carried out according to the protocol described above.

For all compounds, percentage populations were calculated on the basis of ΔE and ΔG values, using Boltzmann statistics and $T = 298$ K. Due to their similarity, only ΔE values were taken into further considerations.[46]

2.5. The Rotational Strength Calculations. To test which combination of functional/basis set performs better in the case of calculations

(39) Boyd, D. R.; Sharma, N. D.; Hand, M. V.; Kerley, N. A.; Dalton, H.; Chima, J.; Sheldrake, G. N. *J. Chem. Soc., Chem. Commun*. **1993**, 974−976.
(40) Boyd, D. R.; Sharma, N. D.; Byrne, B.; Hand, M. V.; Malone, J. F.; Sheldrake, G. N.; Blacker, J.; Dalton, H. *J. Chem. Soc., Perkin Trans. 1* **1998**, 1929−1933.
(41) Boyd, D. R.; Sharma, N. D.; Bowers, N. I.; Duffy, J.; Harrison, J. S.; Dalton, H. *J. Chem. Soc., Perkin Trans. 1* **2000**, 1345−1350.
(42) Resnick, S. M.; Torok, D. S.; Gibson, D. T. *J. Org. Chem.* **1995**, *60*, 3546−3547.
(43) Arvinte, T.; Bui, T. T. T.; Dahab, A. A.; Demeule, B.; Drake, A. F.; Elhag, D.; King, P. *Anal. Biochem*. **2004**, *332*, 47−57.
(44) Frisch, M. J.; Trucks, G. W.; Schlegel, H. B.; Scuseria, G. E.; Robb, M. A.; Cheeseman, J. R.; Zakrzewski, V. G.; Montgomery, J. A., Jr.; Stratmann, R. E.; Burant, J. C.; Dapprich, S.; Millam, J. M.; Daniels, A. D.; Kudin, K. N.; Strain, M. C.; Farkas, O.; Tomasi, J.; Barone, V.; Cossi, M.; Cammi, R.; Mennucci, B.; Pomelli, C.; Adamo, C.; Clifford, S.; Ochterski, J.; Petersson, G. A.; Ayala, P. Y.; Cui, Q.; Morokuma, K.; Salvador, P.; Dannenberg, J. J.; Malick, D. K.; Rabuck, A. D.; Raghavachari, K.; Foresman, J. B.; Cioslowski, J.; Ortiz, J. V.; Baboul, A. G.; Stefanov, B. B.; Liu, G.; Liashenko, A.; Piskorz, P.; Komaromi, I.; Gomperts, R.; Martin, R. L.; Fox, D. J.; Keith, T.; Al-Laham, M. A.; Peng, C. Y.; Nanayakkara, A.; Challacombe, M.; Gill, P. M. W.; Johnson, B.; Chen, W.; Wong, M. W.; Andres, J. L.; Gonzalez, C.; Head-Gordon, M.; Replogle, E. S.; Pople, J. A. *Gaussian 98 and 03*; Gaussian, Inc.: Pittsburgh, PA, 2001.
(45) *CaChe Ws Pro 5.0*; Fujitsu Ltd.
(46) A very recent paper (Lattanzi, A.; Viglione, R. G.; Scettri, A.; Zanasi, R. *J. Phys. Chem. A* **2004**, *108*, 10749) points out the need of using ΔG values rather than ΔE values for calculation of conformer distributions. However, we note that Boltzmann distributions based on ΔE values are well established in the literature. See, for example: (a) Voloshina, E.; Raabe, G.; Estermeier, M.; Steffan, B.; Fleischhauer, J. *Int. J. Quantum Chem.*

of CD spectra of benzene *cis*-dihydrodiols, three different functionals (B3LYP, mPW1PW91, and BHandHLYP) with an increasing fraction of HFXC (20, 25, and 50%, respectively) have been employed. The toluene *cis*-dihydrodiol **1b(*P*)** was selected as a model molecule to test calculations because of its structural similarity to the parent benzene *cis*-dihydrodiol **1a** and the availability of experimental CD data. The lowest-energy conformer **1b(*P*)** was assumed to contribute significantly to the CD spectrum; so in the test computations, the contribution of the higher-energy **1b(*M*)** conformer was omitted.

The results obtained by the TD-DFT computations were compared to those obtained with the CIS method. The CIS and TD-DFT (B3LYP and mPW1PW91) methods were used in conjunction with basis sets ranging from rather small without diffuse functions (6-31g(d), 155 contracted functions) up to cc-pVTZ (410 contracted functions). The BHandHLYP functional was used only in combinations with the 6-311++g(2d,p) basis set.

Selected results are collected in Table A in the Supporting Information, whereas Figure A (see Supporting Information) shows the CD spectra of **1b(*P*)** calculated by the different methods. For clarity, all spectra calculated by the CIS method were shifted to 278 nm to fit the experimental absorption band. Generally, all methods predicted correctly the sign of the lowest-energy transition, but differences were observed in the calculated excitation energies. In the case of the mPW1PW91 and B3LYP functionals, there are only small differences in the calculated transition energies, due to a similar amount of HFXC (25 and 20%, respectively). Increasing HFXC to 50% (BHandHLYP) caused a shift of the calculated transition into a higher-energy region, whereas the CIS method overestimated the transition energy regardless of the basis set used.

The calculated spectra in relation to the experimental spectrum of **1b** show changes depending on the method used. The TD-DFT method in conjunction with the basis sets having no diffuse functions overestimated the rotatory strength of the second transition and underestimated the rotatory strengths of the transitions at shorter wavelengths. Addition of diffuse functions significantly improved the shapes of the calculated CD curves. The addition of the diffuse functions to the double-ζ basis set is apparently more important than upgrading to a triple-ζ basis (as in the triad: cc-pVDZ, aug-cc-pVDZ, cc-pVTZ). This observation is in good agreement with the results obtained by Lynch et al.[47] who suggest additionally that diffuse functions are much more important for DFT than for Hartree−Fock calculations. The addition of diffuse functions is known to improve the CIS calculations of Rydberg excited states. Excitation to a Rydberg state involves a very diffuse terminating orbital, whereas states which are termed "valence" are less diffuse. This distinction can be vague since some valence states are said to possess Rydberg character.[48] Benzene *cis*-dihydrodiols **1a**−**1f**, *trans*-dihydrodiol **4a**, cyclohexadienes **3a**−**3f** and dihydrophenol **4b** have the lowest-energy transitions involving only HOMO and LUMO orbitals. Transitions at higher excitation energies involve occupied orbitals of an energy lower than HOMO and virtual orbitals of an energy higher than LUMO. The CIS method reproduced the CD sign of the lowest-energy transition well, but not the experimental transition energy. The TD-DFT methods in conjunction with the basis sets having no diffuse functions overestimated the rotatory strengths for the transition around 240 nm. On the other hand, addition of diffuse functions caused an underestimation of the rotatory strength of the transition around 240 nm, whereas the CIS method predicted an incorrect sign for this transition rotational strength. Although each experimental spectrum was reproduced well by both B3LYP and mPW1PW91 hybrid functionals in conjunction with the basis sets augmented with diffuse functions, still better overall agreement was obtained with the use of mPW1PW91 hybrid functional and 6-311++g(2d,p) basis sets. This method was subsequently used for the calculation of the spectra of **1a**−**1f**, **3a**−**3f**, **4a**, and **4b**.

Scheme 2. Diastereomeric *P* and *M* Conformations of *cis*-Dihydrodiols **1** and their Acetates **2**

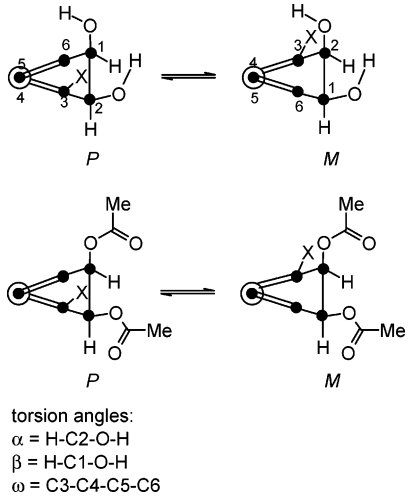

It is well-known that the mPW1PW91 hybrid functional generally provides results which are close or even better than those obtained with the widely used B3LYP method, both for the ground as well as for the excited states.[23,49] This functional provides especially good results for difficult cases, such as those involving van der Waals and covalent interactions.[50]

The computed oscillator strengths and rotational strengths were converted to UV and CD spectra by fitting to Gaussian shape absorption curves. No correlation for the medium dielectric constant was implemented.

2.6. Single-Crystal X-ray Diffraction Analyses. These were performed on *cis*-dihydrodiol metabolites **1c** and **1d** at 150(2) K on a Bruker CCD area-detector diffractometer using graphite-monochromated Mo Kα radiation ($\lambda = 0.71073$ Å) and ϕ/ω scans. Data reduction was performed with the Bruker SAINT program,[51a] and data were corrected for absorption (SADABS). The structures were solved by direct methods and refined using the XS and XL programs, respectively, within the SHELXTL package.[51b] Non-hydrogen atoms were refined anisotropically using weighted full-matrix least squares on F^2. All hydrogen atoms were located in difference Fourier syntheses but were included in the final cycles at positions calculated from the geometries of the molecules, using the riding model.

3. Results and Analysis

3.1. Geometry Optimization of the Dihydrodiols 1a−1f and 4a. *cis*-Dihydrodiols **1b**−**1f** each exist as an equilibrium mixture of diastereoisomeric diene conformers of *P* and *M* helicity. The *P* and *M* conformers of **1a** are enantiomers (Scheme 2).

Whereas the geometry of the cyclohexadiene ring can be fairly well approximated from the earlier X-ray[18] and computational studies,[15] the precise role of substituent X and the hydroxy groups in shifting the $P \leftrightarrows M$ equilibrium toward either

2004, *100*, 1104. (b) Stephens, P. J.; Devlin, F. J.; Cheeseman, J. R.; Frisch, M. J.; Bortolini, O.; Besse, P. *Chirality* **2003**, *15*, 57. (c) Devlin, F. J.; Stephens, P. J.; Scafato, P.; Superchi, S.; Rossini, C. *J. Phys. Chem. A* **2002**, *106*, 10510.
(47) Lynch, B. J.; Zhao, Y.; Truhlar, D. G. *J. Phys. Chem. A* **2003**, *107*, 1384.
(48) Foresman, J. B.; Head-Gordon, M.; Pople, J. A. *J. Chem. Phys.* **1992**, *96*, 135.
(49) Adamo, C.; Barone, V. *J. Chem. Phys.* **1998**, *108*, 664.
(50) See, for example: (a) Kafafi, S. A. *J. Phys. Chem. A* **1998**, *102*, 10404. (b) Yao, X.-Q.; Hou, X.-J.; Jiao, H.; Xiang, H.-W.; Li, Y.-W. *J. Phys. Chem. A* **2003**, *107*, 9991. (c) Li, Q.; Yin, P.; Liu, Y.; Tang, A. C.; Zhang, H.; Sun, Y. *Chem. Phys. Lett.* **2003**, *375*, 470. (d) Tsuzuki, S.; Lüthi, H. P. *J. Chem. Phys.* **2001**, *114*, 3949.
(51) (a) *SAINT;* Program for Data Collection and Data Reduction; Bruker_AXS: Madison, WI, 1998. (b) *SHELXTL*, version 5.0; A System for Structure Solution and Refinement; Bruker_AXS: Madison, WI, 1998.

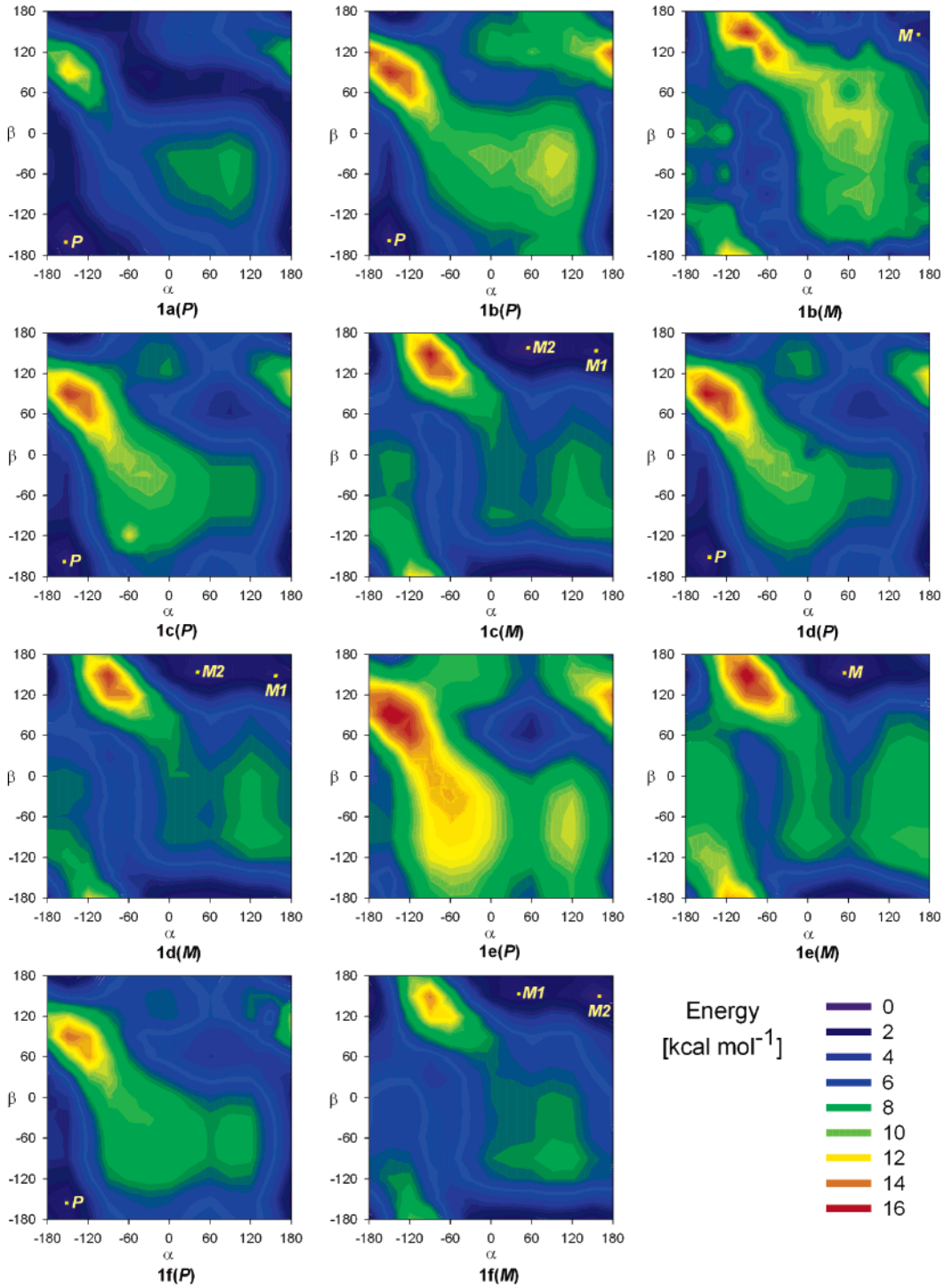

Figure 1. Computed PES for *P* and *M* conformations of **1a**−**1f**. The coordinates belonging to the low-energy conformers are labeled as *P*, *M1*, and *M2* (lower-energy conformer *M* is labeled *M1*).

side remained obscure at the outset of this study. It could be argued that alkyl X substituents favor the *M* conformer with an axial OH group next to the X group due to steric repulsion (for the absolute configuration, as shown in Scheme 2). On the other hand, heteroatom X substituents could shift the equilibrium toward the *P* conformer, with the equatorial OH group engaged in intramolecular hydrogen bonding with the proximate polar X group. A further goal of our computational study was to determine the preferred conformation and hydrogen bonding pattern for each of the two hydroxy groups in different structural (X substituent) and conformational (*P*, *M*) arrangements. Intramolecular hydrogen bonding, if any, could provide a strong conformational bias to one of the low-energy conformers.

The torsion angles necessary to define the rotamers due to the rotation of the C−O bonds were defined as α for H−C2−O−H and β for H−C1−O−H atom chains (see Scheme 2). The DFT calculation of the PES as a function of α and β for each of the two helical (*P*, *M*) conformations of *cis*-dihydrodiols **1a**−**1f** yielded rather surprising but consistent results (Figure 1).

It can be seen that the rotation of each hydroxy group around the C−O bond has a profound effect on the PES of the molecules. The PES shapes for the dihydrodiols are distinctive

for the substitution pattern. The conformations of the parent molecules **1a** and **4a** reach higher energies along the diagonals connecting $\alpha = -180°$, $\beta = 180°$ and $\alpha = 180°$, $\beta = -180°$. Similar PES are displayed by dihydrodiols **1c**, **1d**, and **1f** bearing a heteroatom substituent and also, to some extent, by the methyl- and trifluoromethyl-substituted *P* conformers of dihydrodiols **1b** and **1f**. Within the *P* helical diene family of conformations, the low-energy conformers invariably correspond to the *anti* H−O−C−H bond arrangements, with slight deviation of the OH groups away from the X substituent (α and β in the range of −150 to −160°). The *anti* (*trans*) conformation of H−O−C−H bonds in secondary alcohols was also found to be the most stable in calculations carried out by Polavarapu et al.[52] and Izumi et al.[53]

Hydrogen bond lengths in *cis*-dihydrodiols **1a**−**1e** are calculated to be in the range of 2.136−2.200 Å. There is an indication of a strong intramolecular hydrogen bond O2−H···O1 in the *P* conformers **1b(*P*)**, **1c(*P*)**, **1d(*P*)**, and **1f-(*P*)**, with the equatorial O2−H group as a donor and the O1 atom as an acceptor. The only exception is the trifluoromethyl-substituted dihydrodiol (**1e**) for which no thermally accessible *P* conformer ($\Delta E < 3$ kcal mol^{-1}) was found by the computation. A similar hydrogen bond stabilizes *M* helical conformers **1b(*M*)**, **1c(*M*1)**, **1c(*M*2)**, **1d(M1)**, **1d(*M*2)**, **1e(*M*)**, **1f(*M*1)**, and **1f(*M*2)**, with the equatorial O1−H group as a donor and axial O2 as an acceptor. An additional stabilizing force for *P* and *M* conformers is provided by an axial O−H···π hydrogen bond. In the case of *P* conformers, this is due to O(1)−H···π(6), with the calculated H···C(6) distance of 2.433−2.470 Å, whereas the bonding due to O(2)−H···π(3) is weaker, as a result of a longer H···C(3) distance (2.475−2.496 Å). The effect of C−H···π bonding with the participation of an axial methyl group on the conformational and chiroptical properties of monoalkenes and dienes has been discussed.[54] Details of the structures of the low-energy *P* and *M* conformers are shown in Figure 2 and Table 1.

The *M* helical conformers can be subdivided into two types. One type (middle column in Figure 2) refers to *anti* rotamers of both H−O−C−H bond systems (*anti*, *anti*), as in the case of *P* (left column in Figure 2), but with positive values of α and β in the range of 153−160°. The second type (right column in Figure 2) is accessible only for compounds bearing a polar X substituent (Br, F, CF_3, CN). The O2−H bond is now arranged parallel to the C−X bond due to the stabilizing dipole−dipole interaction. Consequently, the H−C2−O−H bond arrangement is no longer *anti* but *syn* (angle α in the range of 46−56°). Conformers of this (*syn*, *anti*) group are characterized by slightly shorter (0.02−0.03 Å) intramolecular hydrogen bonds (2.150−2.169 Å) compared to those of *anti*, *anti M* conformers (2.185−2.200 Å). The distance between the O2−H proton and substituent X is very different; the longest (3.70 Å) is the H−N distance in conformer **1f(*M*1)**, followed by H−Br (3.20 Å) distance in **1c(*M*2)** and H−F (2.91 Å) in **1d(*M*2)**. Only for **1e(*M*)** does the distance H−F (2.41 Å) and O−H···F geometrical arrangement support the notion of conformer stabilization by an intramolecular O2−H···F hydrogen bond.

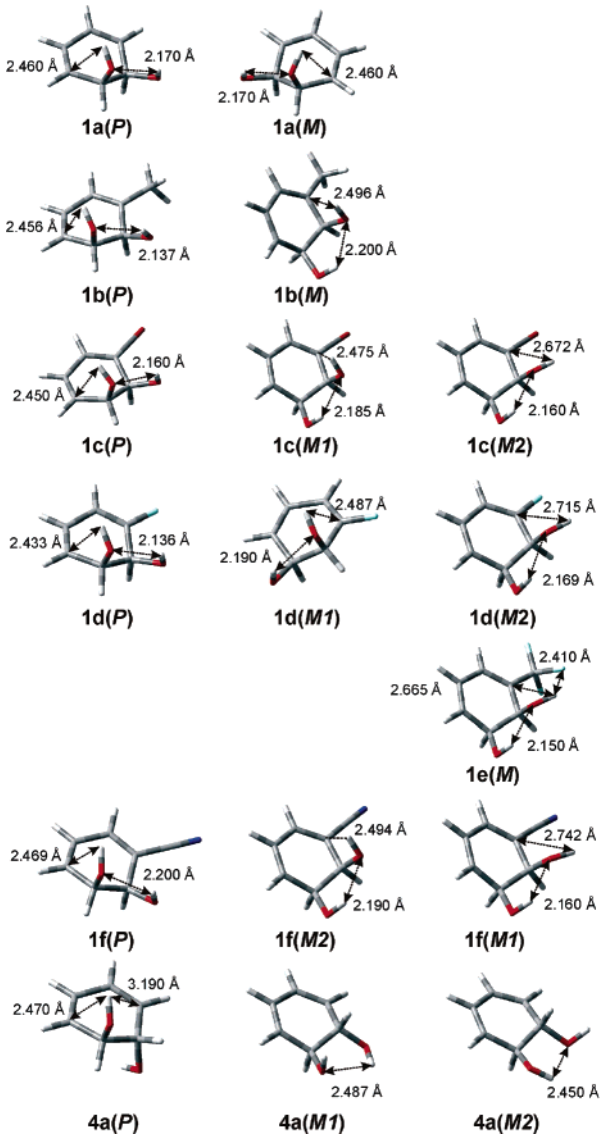

Figure 2. Computed low-energy conformers of dihydrodiols **1a**−**1f** and **4a**, arranged in columns according to structural similarity, with intramolecular hydrogen bonds shown.

The organic fluorine atom accepts a hydrogen bond with difficulty,[55] but the case discussed here may be exceptional due to the favorable geometry and intramolecular character of the interaction between a soft hydrogen donor and a hard fluorine acceptor.

There is some regularity observed with regard to the computed energies of the low-energy conformers of **1a**−**1f**. For **1e**, a single *M* conformer is thermally accessible. In the remaining cases, the conformers are distributed more evenly (see Table 1), but with the preference for either *P* (nonpolar Me substituent) or *M* (polar Br, F, and CN substituents).

Nevertheless, ΔE differences within the chosen energy window do not exceed 0.7 kcal mol^{-1} for a given compound; therefore, all of these dihydrodiol conformers in Table 1 contribute significantly to the chiroptical properties of the bulk compounds. Within the family of heteroatom-substituted dihydrodiols **1c**, **1d**, and **1f**, an interesting difference between

(52) Wang, F.; Polavarapu, P. L. *J. Phys. Chem. A* **2000**, *104*, 10683−10687.
(53) Izumi, H.; Yamagami, S.; Futamura, S.; Nafie, L. A.; Dukor, R. K. *J. Am. Chem. Soc.* **2004**, *126*, 194−198.
(54) Araki, S.; Seki, T.; Sakakibara, K.; Hirota, M.; Kodama, Y.; Nishio, M. *Tetrahedron: Asymmetry*, **1993**, *4*, 555−574.
(55) (a) Dunitz, J. D.; Taylor, R. *Chem.—Eur. J.* **1997**, *3*, 89−98. (b) Desiraju, G. R. *Acc. Chem. Res.* **2002**, *35*, 565−573.

Table 1. Calculated B3LYP/6-311++g(d,p)//B3LYP/6-31++g(d,p) Relative Energies (ΔE) and Structural Parameters (ω, α, β, and μ) for Low-Energy Conformers of **1a**−**1f**, **4a**, and **4b**[a]

conformer	ΔE (ΔG) [kcal mol^{-1}]	population[b] [%]	ω [deg]	α [deg]	β [deg]	μ [D]	f (λ_{max}) [nm]	R [$\times 10^{-39}$ esu^2 cm^2]
1a(*P*)	0.00 (0.00)	50 (50)[c]	11	−152	−160	2.75	0.083 (278)	4.62
1b(*P*)	0.00 (0.00)	63 (64)	10	−150	−158	2.37	0.135 (281)	8.38
1b(*M*)	0.31 (0.34)	37 (36)	−11	165	154	2.76	0.115 (281)	−2.22
1c(*P*)	0.45 (0.65)	22 (14)	7	−156	−158	3.25	0.181 (294)	5.46
1c(*M1*)	0.00 (0.02)	47 (42)	−11	161	154	2.57	0.147 (295)	2.30
1c(*M2*)	0.23 (0.00)	32 (44)	−11	54	160	1.35	0.153 (292)	0.34
1d(*P*)	0.36 (0.51)	27 (18)	9	−154	−154	3.42	0.095 (279)	6.66
1d(*M1*)	0.00 (0.00)	50 (42)	−11	162	153	2.51	0.081 (279)	−4.18
1d(*M2*)	0.45 (0.02)	23 (40)	−9	47	160	1.16	0.085 (278)	−5.61
1e(*M*)	0.00 (0.00)	∼100 (∼100)	−11	56	159	1.65	0.117 (281)	−2.29
1f(*P*)	0.64 (0.97)	15 (11)	11	−155	−160	5.92	0.188 (298)	−2.57
1f(*M1*)	0.00 (0.00)	47 (58)	−10	46	159	2.70	0.199 (302)	4.08
1f(*M2*)	0.12 (0.37)	38 (31)	−11	161	153	4.61	0.180 (303)	6.23
4a(*P*)	0.70 (1.24)	17 (6)	8	−164	−164	3.16	0.058 (275)	19.54
4a(*M1*)	0.00 (0.00)	57 (58)	−13	68	−171	2.31	0.073 (284)	5.70
4a(*M2*)	0.47 (0.28)	26 (36)	−13	62	−47	2.21	0.083 (278)	2.68
4b(*P*)	0.00 (0.00)	92 (88)	10	−168		1.69	0.128 (261)	12.63
4b(*M*)	1.45 (1.17)	8 (12)	−13	−178		1.72	0.099 (275)	5.57

[a] Lowest-energy transition oscillator strengths (f) and rotational strengths (R) are calculated at the mPW1PW91/6-311++g(2d,p) level of theory. [b] In parentheses are populations calculated on the basis of ΔG values. [c] The other 50% is due to enantiomeric *M* conformer.

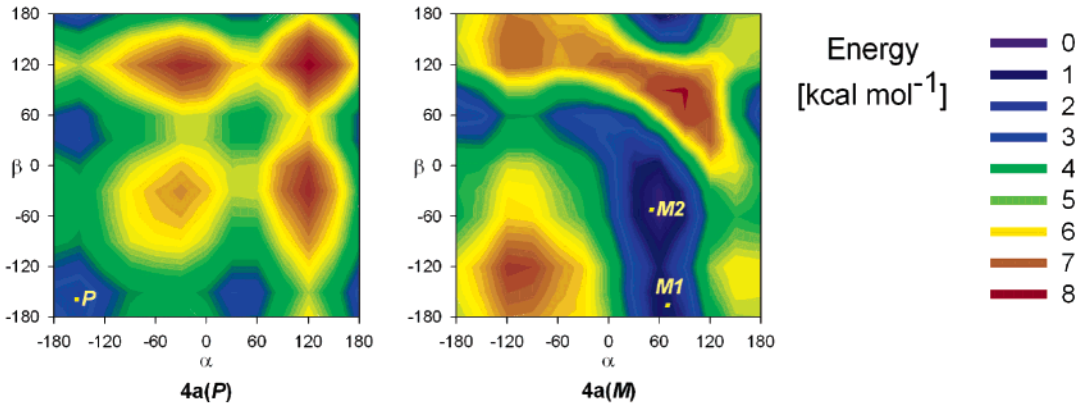

Figure 3. Computed PES for *P* and *M* conformations of **4a**.

computed dipole moments of the low-energy conformers is observed. The largest value of the dipole moment is found for the *P* conformers, the lowest for the third column *M* conformers.

The high value of the dipole moment computed for the *P* conformers seems to indicate the participation of the axial OH group at C1 in the interaction with the diene π electrons at C6. In fact, (O)H···π distances are in the range of 2.43−2.49 Å, shorter for *P*, longer for *M* conformers.

The lowest-energy *M1* conformer of *trans*-diol **4a** is the diequatorial one, with a 2.49 Å intramolecular O−H···O bond. The arrangement of the H−C−O−H bonds with the acceptor oxygen atom is *anti*, and with the hydrogen donor is *syn*. The energy of the molecule increases upon rotation of the former bond system to *syn* (conformer *M2*). The diaxial *P* conformer is of still higher energy (ΔE = 0.70 kcal mol^{-1}), with no intramolecular hydrogen bond (Table 1 and Figure 3).

3.2. X-ray Diffraction Determined Structures of Substituted Benzene *cis*-Dihydrodiols. To examine the molecular conformations in the solid state, single-crystal X-ray analyses have been performed on the bromo- (**1c**) and fluorobenzene (**1d**) bioproducts. The analyses confirmed both compounds as enantiopure, and application of the anomalous dispersion X-ray method to the analysis of **1c** independently confirmed the absolute configuration for this compound as (1*S*). Both compounds exist exclusively as the *M* conformers in the solid state, and thus the OH groups on C2 and C1 are axial and equatorial, respectively (Figure 4; see also Scheme 2). The packing of molecules, however, differs between the two compounds, with *cis*-dihydrodiol **1d** having two crystallographically independent, but conformationally indistinguishable, molecules in the unit cell. In metabolite **1c**, the torsion angles α, β, and ω (as defined in Scheme 2) are +6.8, +57.4, and −11.6°, respectively. In compound **1d**, the corresponding angles for the two crystallographically independent molecules are −62.7/−62.6, +63.9/+63.9, and −10.0/−10.2°, respectively. The presence of two independent molecules in the unit cell is likely to be due to optimizing the intermolecular hydrogen bonding required for crystal growth.

Figure 4. X-ray diffraction determined structures of substituted benzene *cis*-dihydrodiols.

3.3. Computed and Experimental Electronic Transitions. The computed lowest-energy transitions and their oscillator

Table 2. Calculated B3LYP/6-311++g(d,p)//B3LYP/6-31++g(d,p) Torsion Angles (ω) of the Lowest-Energy *P* Conformers of **3a**−**3f**[a]

	ω [deg]	$f(\lambda_{max})$ [nm]	R [10^{-39} esu^2 cm^2]
3a	14	0.117 (268)	0.29
3b	14	0.163 (272)	2.47
3c	13	0.201 (281)	−1.23
3d	13	0.113 (267)	2.89
3e	14	0.158 (272)	0.75
3f	14	0.246 (295)	−3.94

[a] Oscillator strengths (*f*) and rotational strengths (*R*) of the lowest-energy transition were calculated at the mPW1PW91/6-311++g(2d,p) level of theory.

strengths (λ_{max} and *f*) for each of the low-energy conformers **1a**−**1f**, **4a**, and **4b** are given in Table 1. The lowest-energy singlet transition was the center of attention being of defined character, well-separated from other electronic transitions, and previously used for spectra−structure correlations of numerous *cis*-dienes.[10] Higher-energy (shorter wavelength) transitions obtained by computation (see Supporting Information) are of complex character (see below).

According to our computations and previously collected knowledge, the lowest-energy singlet transition in cyclohexadienes is primarily of the $\pi-\pi^*$-type, involving HOMO−LUMO orbitals of the system. This is the only component of the computed transitions of 1,3-cyclohexadiene (**3a**) and its monohydroxy derivative (**4b**) in the longest wavelength absorption envelope. However, a contribution from a HOMO(−1)−LUMO transition is found for dihydroxy-substituted 1,3-cyclohexadiene derivatives, including dihydrodiols **1a**−**1f** and **4a** from this study. This transition is of $\sigma-\pi^*$ character, as previously computed for 5-methyl-1,3-cyclohexadiene,[14] and involves the C−O bond(s) of the dihydrodiol moiety. In general, the presence of the C−O bond lowers the excitation energy of the diene, more in the case of equatorial rather than axial C−O bonds, producing a shift to longer wavelengths (cf. Tables 1 and 2).

A comparison of the computed (Tables 1 and 2) and experimental data (Table 3) shows the significant effect of the X substituent on the λ_{max} and ϵ_{max} of the diene chromophore. Both values increase in the order F < CF_3 < Me < Br < CN. The effect of the cyano substituent is best explained by conjugation with the additional π orbitals. Transition energy and probability in the other cases appear to be correlated with the acceptor/donor properties of the substituent, with the case of the bromine substituent being less clear, however. A study of the solvent effect (Table 3) reveals a significant effect of solvent polarity. In all cases **1b**−**1f**, the λ_{max} values decrease 4−6 nm with increased solvent polarity (cyclohexane → water).

In addition, the computed λ_{max} values for isolated molecules are higher than the experimental values. Apparently, a *reverse* solvent effect on the $\pi-\pi^*$ transition (blue shift with increased solvent polarity) can be rationalized by the presence of the intramolecular O−H···π hydrogen bond in a nonpolar environment (see computed structures in Figure 2), which is broken in aqueous solution. This O−H···π hydrogen bond is expected to stabilize the excited state of the diene chromophore. Further support is obtained from the inspection of data for *O*-acetylated derivatives **2a**−**2d** (Table 4); in the absence of the OH groups, the λ_{max} values are blue shifted (3−5 nm) compared to the data for **1b**−**1f** (in acetonitrile solution).

Table 3. Experimental CD and UV Data for *cis*-Dihydrodiols **1b**−**1f** in Cyclohexane, Dichloromethane, Acetonitrile, and Water Solutions

		First Transition		Second Transition
compound	solvent	UV, ϵ (λ nm)	CD, $\Delta\epsilon$ (λ nm)	CD, $\Delta\epsilon$ (λ nm)
1b	C_6H_{12}	5075 (270.6)	+2.88 (273)	−5.6 (211.8)
(1*S*,2*R*)	CH_2Cl_2	5162 (270)	+1.05 (277)	−ve
	CH_3CN	5050 (267)	+0.88 (276.5)	−3.4 (214.5)
	H_2O	5150 (265.5)	+0.55 (280.5)	−4.0 (214)
			−0.31 (248)	
1c	C_6H_{12}	6674 (278.6)	+1.53 (283)	−7.7 (214)
(1*S*,2*S*)	CH_2Cl_2	6720 (277)	+2.23 (279.5)	−ve
	CH_3CN	6600 (274.5)	+2.22 (279.5)	−8.6 (217.5)
	H_2O	6665 (272.6)	+2.01 (279.5)	−9.9 (216)
1d	C_6H_{12}	3915 (264)	+0.05 (297)	−1.7 (215)
(1*S*,2*S*)			−2.50 (262)	
	CH_2Cl_2	3810 (263.5)	+0.05 (297)	−ve
			−1.81 (261)	
	CH_3CN	3837 (260)	−2.43 (257)	−2.2 (213.5)
	H_2O	3880 (260)	−2.92 (257)	−1.7 (211)
1e	C_6H_{12}	3120 (268.5)	−2.58 (264.5)	−4.2 (224)
(1*S*,2*R*)	CH_2Cl_2	3080 (266.4)	−1.51 (265)	−3.1 (221.5)
	CH_3CN	3115 (265.5)	+0.10 (298.5)	−4.5 (224.5)
			−1.41 (258)	
	H_2O	3185 (264)	+0.23 (293)	−4.6 (217.5)
			−0.66 (257.5)	
1f[a]	CH_2Cl_2	6564 (285)	+2.00 (285.5)	−ve
(1*S*,2*R*)			+1.7 (246)	
	CH_3CN	6510 (284)	+2.27 (286.5)	−ve
			+1.3 (258)	
	H_2O	6486 (285)	+2.01 (289)	−ve
			+0.98 (253)	

[a] Insufficient solubility in cyclohexane.

Table 4. Experimental CD and UV Data for *cis*-Dihydrodiol Diacetates **2a**−**2d** in Acetonitrile Solution

	First Transition		Second Transition
compound	UV, ϵ (λ nm)	CD, $\Delta\epsilon$ (λ nm)	CD, $\Delta\epsilon$ (λ nm)
2a	4300 (262)	+0.6 (278)	−2.3 (208)
		−0.4 (245)	
2b	4440 (270.5)	−2.5 sh (248)	−13.0 (212)
2c	4200 (257.5)	−4.8 (260)	−2.7 (213)
2d	4220 (260.5)	−6.7 (255)	−4.3 (214.5)

3.4. Computed and Experimental Circular Dichroism Spectra of Dihydrodiols. In this section, the experimental and computed chiroptical data for *cis*-dihydrodiols **1a**−**1f** are compared to account for the distribution of conformers at equilibrium ($P \leftrightarrows M$) and for the rotational strengths of individual conformers (see Table 1). The experimental CD data for dihydrodiols of the same (1*S*) configuration ((1*S*,2*R*) or (1*S*,2*S*), Figure 5 and Table 3) are frequently controlled by overlap cancellations of the bisignate CD curves and show a positive long-wavelength Cotton effect of the first transition for Me (**1b**)-, Br (**1c**)-, and CN (**1f**)-substituted diene chromophores, whereas a negative main Cotton effect is observed for the F (**1d**) and CF_3 (**1e**) diene substitutions. The sign of the underlying Cotton effects is not altered by the solvent used (cyclohexane, dichloromethane, acetonitrile, or water), but the magnitude is. A change in magnitude of the Cotton effect reflects the solution equilibrium between *P* and *M* conformers. In general for the whole series, a positive CD is found in the first absorption region peaks at the UV_{max} or at longer wavelength, whereas a negative CD is found either at the UV_{max} or at shorter wavelength. This suggests that the λ_{max} for the *P* conformer is at slightly longer wavelength than λ_{max} for the *M* conformer.

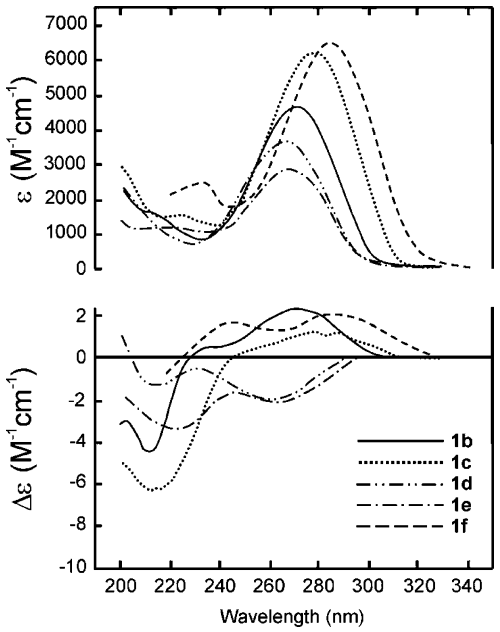

Figure 5. Experimental CD and UV curves for *cis*-dihydrodiols **1b**−**1e** (in cyclohexane) and **1f** (in dichloromethane).

Dihydrodiol **1b** in water solution gives a positive Cotton effect at 280 nm, accompanied by a weaker negative one at 248 nm, whereas negative Cotton effects of **1d** and **1e** are associated with very weak positive long-wavelength maxima in cyclohexane or dichloromethane (**1d**) and acetonitrile or water (**1e**) solutions. Significantly, short-wavelength (208−225 nm) Cotton effects for all of these dienes are consistently negative. The experimental sign of the long-wavelength Cotton effect may appear difficult to correlate with dihydrodiol absolute configuration; however, the computed results provide a clue to the puzzling CD data.

Dihydrodiol **1b** (as well as **1a**) presents a rotational strength (*R*) with a sign that correlates with diene helicity, including the axial C1−O bond. The lower-energy *P* conformer has a much higher (4-fold) rotational strength compared to that of the *M* counterpart; hence, the net Cotton effect is positive, as in the experiment. In water solution, a negative CD band appears at 248 nm due to increased population of the *M* conformer of **1b** in polar solution, as a result of breaking the O−H···π hydrogen bond and stabilizing the *P* conformer.

In the bromo derivative **1c**, all conformers (*P* and *M*) are characterized by a positive net Cotton effect, which is, therefore, independent of conformer equilibrium and positive, as in the experiment.

The fluoro derivative **1d** presents a CD in accord with diene helicity, as in the case of the *cis*-dihydrodiol **1b**. However, in this case, the distribution of conformers is in favor of *M* species, and a net negative *R* value is calculated corresponding to a negative experimental Cotton effect.

The trifluoromethyl derivative **1e** presents the only conformer of *M* helicity, which was found by computation to have a negative CD, again in agreement with the measured negative Cotton effect in nonpolar solvents. In polar water solution, experimental data suggest the presence of a *P* conformer for **1e** with positive CD, apparently resulting from the breaking of the O−H···F hydrogen bond stabilizing the **1e**(***M***) conformer.

Table 5. CD Data for Other *cis*-Dihydrodiols **1** in Acetonitrile Solution

compound		X	Δε (nm)	
1g	(1*S*,2*R*)	*n*-Pr	+1.20 (273)	−3.8 (216)
1h	(1*S*,2*R*)	*i*-Pr	+1.80 (273)	−3.5 (215)
1i	(1*S*,2*R*)	*n*-Bu	+0.83 (272)	−3.2 (213)
1j	(1*S*,2*R*)	*i*-Bu	+2.33 (273)	−3.1 (218)
1k	(1*S*,2*R*)	*s*-Bu	+0.67 (278)	−3.5 (219)
1l	(1*S*,2*R*)	*t*-Bu	+3.10 (272)	−1.7 (219)
1m	(1*S*,2*R*)	*n*-C_5H_{11}	+2.27 (276)	−3.0 (219)
1n	(1*S*,2*R*)	CH_2-*t*-Bu	+6.45 (270)	−5.0 (218)
1o	(1*S*,2*R*)	CH_2CN	+1.77 (264)	−1.8 (205)
1p	(1*S*,2*R*)	COMe	+7.3 (298)	−9.7 (231)
1q	(1*S*,2*R*)	COOMe	+1.9 (298)	−2.6 (220)
1r	(1*S*,2*S*)	Cl	+1.4 (280)	−5.5 (218)
1s	(1*S*,2*S*)	I	+3.2 (282)	−8.6 (235)
1t	(1*S*,2*S*)	OMe	+0.34 (298)	−1.7 (218)
			−0.36 (263)	
1u	(1*S*,2*S*)	OEt	+0.44 (297)	−1.9 (219)
			−0.29 (262)	
1v	(1*S*,2*S*)	SMe	+0.50 (304)	−3.5 (209)
			−0.04 (267)	
1w	(1*S*,2*S*)	SEt	+1.4 (311)	−7.8 (209)
			+1.1 (250)	
1x	(1*S*,2*S*)	S*i*-Pr	+0.9 (323)	−7.5 (209)
			+1.8 (255)	
1y	(1*S*,2*S*)	S*t*-Bu	+1.1 (330)	−6.0 (215)[a]
			+7.5 (272)	
1z	(1*S*,2*R*)	Ph	+6.5 (314)	

[a] Shoulder.

The computed rotational strength of the individual conformers of **1f** is of considerable interest, as the sign of *R* is *opposite* to that expected based upon diene helicity. This result provides a computational foundation for the previously noted exception to the *Diene Helicity Rule* induced by the cyano group.[13] Since the computed population of *M* conformers of **1f** amounts to 85%, the net computed rotational strength is positive, again in agreement with the experimentally determined positive Cotton effect.

A number of *cis*-dihydrodiol metabolites (**1g**−**1z**) of similar (1*S*) configuration obtained from the corresponding benzene derivatives have been characterized by CD spectra (Table 5). In view of present findings, the experimental CD spectra confirm the (1*S*,2*R*) configuration assigned to various 3-alkyl derivatives (**1g**−**1n**) on the basis of their positive long-wavelength Cotton effect, as in the case of **1b**. On the other hand, the (1*S*,2*S*)-3-OR *cis*-dihydrodiol derivatives (**1t** and **1u**) exhibit distinct bisignate long-wavelength Cotton effects due to complex conformational equilibria.[56] π-Conjugated derivatives, with the carbonyl (**1p** and **1q**) or aryl (**1z**) substituents at C3, display a positive long-wavelength Cotton effect, apparently in analogy to a positive Cotton effect of the π-conjugated cyanodiene **1f**.

Finally, for comparison purposes, rotational strengths of the conformers of the *trans*-dihydrodiol **4a** have been calculated. For a given absolute configuration (1*S*), all low-energy conformers shown in Table 1 are characterized by a positive *R* value of differing magnitude. A very high *R* value (19.54×10^{-39} esu^2 cm^2) was computed for the *P* conformer with diaxial allylic hydroxy groups. It was more than 3 times higher compared to that of the most abundant *M1* conformer ($R = 5.70 \times 10^{-39}$ esu^2 cm^2), in which the hydroxy groups are diequatorial.[57] The

(56) Preliminary computational data for the 3-methoxy *cis*-dihydrodiol **1t** indicate the presence of two *P* and one *M* conformers in the equilibrium. In the lowest-energy *P* conformer, the stabilizing effect is due to a bifurcated O1−H···O2−H···O(Me) hydrogen bond.

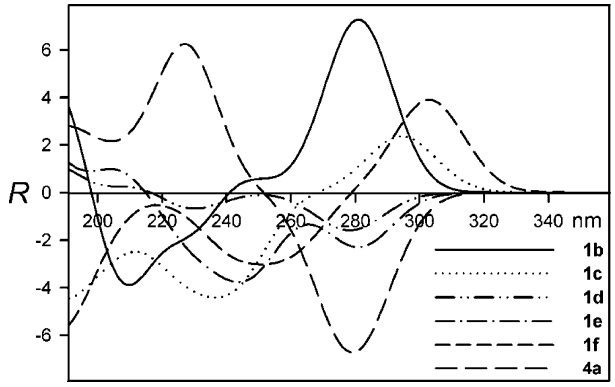

Figure 6. Computed CD spectra ($\times 10^{-39}$ esu^2 cm^2) of dihydrodiols **1b**−**1f** and **4a** after Boltzmann averaging due to conformer population.

diequatorial *M1* and *M2* conformers differ mainly by the preferred relative orientation (angle β) of one hydroxy group. In the case of *M1*, angle β corresponds to the *anti* arrangement, and in the case of *M2*, it is *syn*; yet the value of *R* is double that of the former. Thus, the rotational strength of the lowest-energy transition Cotton effect of **4a** is positive, regardless of the conformer population. This computational result is in agreement with the earlier experimental data[18] from which a much higher (positive) rotational strength was assigned to the diaxial conformer compared to that of the diequatorial one.

Finally, the computed Boltzmann weighted CD spectra of dihydrodiols **1b**−**1f** and **4a** are shown in Figure 6 (for direct comparison with the experimental CD spectra of individual compounds, see Supporting Information).

A good overall agreement has now been found between the experimental (Figure 5 and ref 18) and computed signs of the Cotton effects. This correlation applies not only to the long-wavelength Cotton effects but also to those in the range of 210−225 nm, which have not been invoked previously for absolute configuration−spectra correlation.

A comparison of the CD spectra of *cis*-dihydrodiols (**1a**−**1d**) and their diacetates (**2a**−**2d**) (Table 4) indicates that the CD spectra of diacetates **2a**−**2d** show two Cotton effects in the range of 200−300 nm, as do the CD spectra of the parent dihydrodiols **1b**−**1e**. The difference between the long-wavelength Cotton effects of the diacetates **2a**−**2d** and diols **1b**−**1e** can be accounted for by adding a negative contribution to the Cotton effect of the corresponding dihydrodiols **1b**−**1e**. Thus, the Cotton effect of the diacetate **2a** is bisignate, rather than positive, as in the case of diol **1b**, whereas the Cotton effect for **2b** is negative, in contrast to the positive observed for **1c**. In the case of diacetates **2c** and **2d**, negative Cotton effects are more intense than those of the corresponding diols **1d** and **1e**.

In the absence of hydrogen bonding in diacetates, the conformer equilibrium ($P \leftrightarrows M$) (C═O bond *syn* to C−H bond; see Scheme 2) is shifted in the direction of the *M* conformer. This provides a negative contribution to the long-wavelength Cotton effect of diacetates **2a**−**2d**. The short-wavelength Cotton effects of diacetates **2a**−**2d** are in all cases negative, as are the corresponding Cotton effects of diols **1b**−**1e**.

4. Discussion

Experimental CD and X-ray diffraction data, in combination with the results of DFT computations, indicate that the conformational and chiroptical properties of dihydrodiol molecules are intimately dependent on the interplay of interactions related to the hydroxy groups at C1 and C2 and the substituent X at C3. This includes hydrogen bonding (O−H···O, O−H···π, and O−H···F in **1e**), dipole−dipole interactions, and steric effects, all of which influence the conformational equilibrium between *P* and *M* conformers. The free energy of the dihydrodiol molecule has been found to be strongly dependent on the conformation of the hydroxy groups resulting from rotation around the C−O bonds (see Figure 1). In addition, the conformation of the hydroxy groups influences the rotational strength of the electronic transitions of the dihydrodiol molecules (see Table 1 and Supporting Information). A further complicating factor is the nature of substituent X at C3 of the dihydrodiol molecule; substituents such as Br or CN reverse the rotational strength of the long-wavelength transition for a given diene conformer (see Tables 1 and 2). It is therefore justified to say that both the conformational and the chiroptical properties of dihydrodiols **1b**−**1f** are governed by the heteroatom substituents X and hydroxy groups. A concise characterization of dihydrodiols **1b**−**1f** is presented in Table 6.

Table 6. Characterization of Dihydrodiols **1b**−**1f** from Both Computational and Experimental Data (λ_{max}, ϵ_{max}, and *R* data for the lowest-energy transition)

X	λ_{max}	ε_{max}	conformer population	*R*
CN	↑	↑	*M* > *P*	+ > −
Br			*M* > *P*	+ only
Me			*P* > *M*	+ > −
F			*M* > *P*	− > +
CF_3			*M*	−

The present study indicates that there is no existing empirical model that can fully account for the experimental CD data of all *cis*-dihydrodiols, including the *Diene Helicity* and the *Allylic Chirality Models*. In the *Diene Helicity Model*, the rotational strength contribution from a helical cyclohexadiene chromophore is in any case weak and, in certain cases (Br, CN substituents at C3), does not correlate with the sign of diene torsion angle. In the *Allylic Chirality Model*, the failure results from mutually canceling contributions due to allylic hydroxy groups, both axial and equatorial, in conformers of *P* and *M* helicity. A prudent way to assign the configuration/conformation of a *cis*-dihydrodiol is to critically confront the experimental CD data with the computed rotational strengths of the diene electronic transitions for all contributing conformers. However, it is tempting and possible to offer a simplified model to reconcile the experimental and computational results. First, both experimentally and computationally, all *cis*-dihydrodiols of the (1*S*) configuration (**1a**−**1z**) show a second, *negative* CD band in the region of 240−200 nm. Although the origin of this CD band is not adequately understood, most probably it results from overlap of several transitions of presumably $\sigma-\pi^*$ (or $\pi-\sigma^*$) character. Second, since the computed rotational strength of the long-wavelength transition in nonhydroxylated cyclohexadienes is low (Table 2), an approximate contribution of hydroxy substituents can be obtained by subtracting the rotational strength *R* values of Table 2 from the data of Table 1 for the corresponding conformer. The obtained ΔR values (Table C,

(57) Support for a dominant diequatorial conformation of *trans*-dihydrodiols is obtained from their ^{1}H NMR spectra: $J_{H1,H2} = \sim 10$ Hz.

Scheme 3. Estimated Contributions to Computed R ($\times 10^{-39}$ esu^2 cm^2) of *P* and *M* Conformers

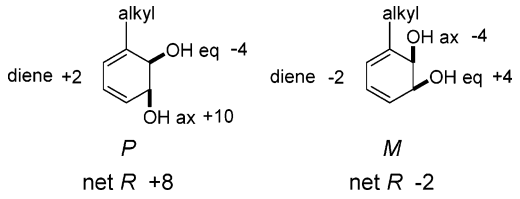

Supporting Information) show a dominant contribution of conformers with the axial hydroxy groups over those with the equatorial ones (**4a** and **4b**), while the sign of the contribution remains unchanged for either conformer in the same configurational series. In *cis*-diols **1a**−**1f**, an axial hydroxy group at C1 (conformer *P*) contributes more strongly than does a hydroxy group at C2 (conformer *M*). For C3−alkyl-substituted dihydrodiols (e.g., **1b** and **1g**−**1n**, such as those in Table 5), the estimated contributions due to individual conformers are shown in Scheme 3.

In the case of the CN-substituted dihydrodiol (**1f**), the hydroxy groups of all conformers contribute weakly to the rotational strength, whereas the parent cyanocyclohexadiene **3f** shows a moderate rotational strength with a sign opposite to that expected based upon diene helicity. The dominating effect of the cyanodiene chromophore obtained by DFT computation provides a rationale for the previously noted abnormal CD behavior of CN-substituted dienes.

The X-ray analyses indicate that neither dihydrodiol **1c** nor **1d** shows intramolecular hydrogen bonding in the solid state. In compound **1d**, a five-membered intramolecular ring involving fluorine is possible, but the hydroxyl hydrogen is pointing away from the fluorine atom in both crystallographically independent molecules. Neither is the fluorine atom involved in intermolecular interaction. Both OH groups in each molecule of *cis*-diols **1d** and in **1c** are involved in intermolecular interactions, as both hydrogen donors and hydrogen acceptors, although the resulting networks are different for the two compounds. In metabolite **1c**, molecules pack to form infinite hydrogen-bonded chains, whereas in compound **1d**, they bond in cross-linked pairs to form a three-dimensional network. In these laboratories, X-ray analyses have been performed on a total of eight monosubstituted benzene *cis*-dihydrodiol compounds (unpublished data). All are enantiopure, with a (1*S*) configuration, and seven of them have exclusively *M* helicity. The single exception (X = SOPh) exists as an equal mixture of *M* and *P* conformers, but with the same configuration. One of these eight compounds, other than **1c**, contains a fluorine atom (X = CH(OH)CF_3), but this shows no intramolecular hydrogen bonding, where a seven-membered ring is possible, and no intermolecular interaction involving fluorine. *Etter's Rules*[58] state that all good proton acceptors (e.g., F) should be used in hydrogen bonding and that six-membered ring intramolecular hydrogen bonds form in preference to intermolecular hydrogen bonds. Despite several attempts, our failure to form suitable crystals of compound **1e** (X = CF_3), in which a six-membered intramolecular hydrogen bond is possible and is predicted by the computational studies, might suggest that intramolecular bonding predominates and thus minimizes the intermolecular bonding needed for crystal growth.

The work reported here for the CD−absolute configuration analysis of *cis*-dihydrodiols is being extended to encompass other disubstituted benzene derivatives.

Acknowledgment. We wish to thank the Committee for Scientific Research (KBN; J.G.), the Foundation for Polish Science (FNP; M.K.), the Queen's University of Belfast (CenTaCat; N.D.S.), and Applied Photophysics (A.F.D.) for support. All calculations were performed at Poznan Supercomputing Center.

Supporting Information Available: Results of testing calculations for **1b(*P*)**; calculated energies of conformers **1a**−**1f**, **4a**, and **4b**; relative contributions of hydroxy substituents to the rotational strength; Cartesian coordinates of all optimized structures; calculated oscillator strengths and calculated rotatory strengths for all optimized structures; crystal data for **1c** and **1d**; experimental CD spectra of **1b**−**1f** and **2a**−**2d** measured in different solvents; a comparison of the experimental and calculated CD spectra for individual dihydrodiols **1b**−**1f**; and a comparison of the length and velocity representations of the CD spectra of the lowest-energy conformers of **1a**−**1f**. This material is available free of charge via the Internet at http://pubs.acs.org.

JA042895B

(58) Etter, M. C. *Acc. Chem. Res*. **1990**, *23*, 120−126.